PCCP

ROYAL SOCIETY OF CHEMISTRY

PAPER

View Article Online
View Journal

Cite this: DOI: 10.1039/d0cp03575k

Vibration mediated photodissociation dynamics of CH_3SH: manipulation of the dynamic energy disposal into products†

Heesung Lee and Sang Kyu Kim *

Received 4th July 2020,
Accepted 30th July 2020

DOI: 10.1039/d0cp03575k

rsc.li/pccp

The S–H bond dissociation dynamics of CH_3SH have been investigated for the S_1–S_0 transition mediated by either the S–H stretching (2608 cm^{-1}) or CH_3 symmetric stretching (2951 cm^{-1}) mode excitation in the S_0 state. The S–H and C–S bond extensions are strongly coupled in the S_1 state through the S_1/S_2 same-symmetry conical intersection, giving the C–S stretching mode excitation of the $CH_3S^\bullet$ fragment during the prompt S–H bond rupture on S_1. In the IR + UV transition mediated by the S–H stretching mode, the vertical transition seems to access the Franck–Condon region where the S–H bond is shortened while the coupling to the C–S bond stretching becomes stronger compared to the case of one-photon UV transition, indicating that the intramolecular vibrational redistribution (IVR) is little activated in S_0. When the IR + UV excitation is mediated by the CH_3 symmetric stretching mode, on the other hand, the Franck–Condon region in S_1 encompasses the enlarged molecular structures with respect to both S–H and C–S bond extensions, presumably due to the rapid IVR in S_0 prior to the vertical transition. This leads to the inverted vibrational state population of the C–S bond stretching mode of the $CH_3S^\bullet$ fragment. This work demonstrates that the reaction dynamics upon the IR + UV excitation of CH_3SH is highly mode dependent and the energy disposal dynamics could be controlled by the manipulation of the Franck–Condon region through the particular vibrational-state mediation in the ground state, shedding new light on the structure–dynamics relationship.

Introduction

The vibration mediated photodissociation dynamics had been extremely successful in the passive control of the reaction in terms of the bond-selective chemistry.[1,2] The reaction control by the vibrational mediation, however, cannot be robustly applied as it relies on the nature of the intramolecular vibrational redistribution (IVR) dynamics in both ground and excited states. Namely, if the rate of energy randomization by IVR exceeds the rate of the excited-state reaction, the initial memory of the molecule given by the optical vibrational excitation is partially or completely washed out. In this regard, IVR is the most critical hurdle to be overcome for the successful bond-selective chemistry.[3–5] Another important dynamic aspect of the vibration mediated photochemistry could be found in terms of the manipulation of the vertical transition. Namely, as the electronic excitation is instantaneous, the optical electronic transition from the particular vibrational states of the ground electronic state would be different from that from the zero-point level in terms of the accessible Franck–Condon (FC) region in the excited state. Namely, using the largely modified FC overlap integrals by the various vibration-mediated optical transitions, the exploration of different phase spaces in the excited state would be plausible. Actually, the double excitation scheme has long been widely and successfully applied in the spectroscopic and/or dynamic characterization of the excited-state chemistry for many decades.[6–15]

Herein, we have explored different phase spaces of the first electronically excited state of CH_3SH by employing the vibration-mediated photodissociation scheme. In the recently reported IR-VUV double excitation experiment on CH_3SH, the Lee group[16] has clearly identified the role of ground state vibrational modes of ν_3 (SH stretching) or ν_2 (CH_3 symmetric stretching) in the Rydberg state excitation and ionization. Even though it was not explicitly stated in their report, the sharply or less-sharply rising edge observed at the vertical ionization threshold of CH_3SH from the IR + VUV double excitation *via* ν_3 or ν_2, respectively,[16] implies that the SH stretching mode might survive IVR whereas the CH_3 symmetric stretching mode may lose its bright character *via* the rapid energy randomization. Motivated

Department of Chemistry, KAIST, Daejeon 34141, Republic of Korea.
E-mail: sangkyukim@kaist.ac.kr

† Electronic supplementary information (ESI) available: 1-, 2-, and 3-color H^+ PHOFEX and TKER distributions, fitting parameters, and the energy correlation plot. See DOI: 10.1039/d0cp03575k

by this observation, we have carried out the IR + UV double excitation experiment using either the ν_2 or ν_3 mode excitation in the ground state. The H atom detachment dynamics occurring on the S_1 state of CH_3SH, using the IR + UV excitation scheme mediated by the ν_2 or ν_3 vibrational mode excitation, has been investigated and the results are compared to those obtained from the direct one-photon UV (Fig. S3–S4, ESI†) excitation.

Photodissociation dynamics of CH_3SH has been both extensively and intensively studied for many years recently.[17–31] According to previous theoretical and experimental works, two distinct C–S and S–H bond dissociation channels have clearly been identified and their dynamics have thoroughly been investigated in terms of the scalar and vector properties of products upon ultraviolet excitation in the 274–202 nm region.[17–31] Briefly, the first electronically excited state ($1^1A''$) is overall dissociative with respect to both the S–H and C–S bond elongation coordinates, though the potential energy surface exhibits a small barrier at short C–S separations, facilitating the preferential prompt S–H bond rupture on the repulsive $1^1A''$ although the thermodynamic bond dissociation energy of the C–S bond is smaller than that of the S–H bond.[28,32–34] The second lowest excited state ($2^1A''$), on the other hand, is calculated to be bound with respect to both S–H and C–S bond extension coordinates. Once excited, however, it is efficiently coupled to the low-lying $1^1A''$ state, giving the final products from either the S–H or C–S bond dissociation event eventually. The coupling of the S–H and C–S bond stretches on both $1^1A''$ and $2^1A''$ is predicted to be strong and much influenced by the vibronic coupling mediated by the same-symmetry conical intersection.[32–34] The theoretically predicted entanglement of the S–H and C–S bond stretching motions in the excited states has been experimentally manifested in the internal state distribution of products.[17–21,25,27–31] Namely, in the translational energy distribution of the H fragment from the S–H bond dissociation, the C–S stretching mode of the $CH_3S^\bullet$ fragment is found to be mainly excited.[17–21,25,27] The translational energy distribution of the nascent $^\bullet CH_3$ fragment in the C–S bond dissociation channel, on the other hand, shows that the SH stretching vibrational mode is highly excited in the $^\bullet$SH co-fragment.[28–31] Particularly, the inverted population of the $^\bullet$SH fragment was found in most cases, suggesting that the nuclear motion along the S–H stretching gets highly excited as the C–S bond rupture takes place during the $2^1A''$–$1^1A''$ vibronic coupling.[28–31]

Methods

A detailed experimental setup had been described in previous works.[32,33] Briefly, the gas mixture (1 wt% CH_3SH in He) was expanded through a nozzle orifice (General Valve series-9) and skimmed through a 1 mm diameter skimmer into vacuum with the backing pressure of 1 atmosphere at the 10 Hz repetition rate. The laser pulse ($\Delta t \sim 6$ ns) in the 263–278 nm range was generated by the frequency doubling of the dye-laser output (Sirah, Cobra-Stretch) pumped by the second harmonic of a Nd:YAG laser (Spectra Physics, Quanta-ray LAB170). Another independently tunable laser pulse in the 216–226 nm region was generated from a dye laser (Lambda Physik, Scanmate II) pumped by the third harmonic (355 nm) of a Nd:YAG laser (Continuum, Surelite-II-10). The reduced-Doppler double excitation scheme was employed.[34–37] For detecting the nascent H photofragment, two counter-propagating UV laser pulses were spatiotemporally overlapped so that the non-resonant (1 + 1′) double excitation matches with the 121.57 nm (82256.8 cm^{-1}) 2s–1s Rydberg transition of H. These UV laser pulses are both used for their distinct one-photon electronic transitions of CH_3SH whereas their combination is used for the ionization of the H atom. The IR laser pulse of 0.2–12 mJ per pulse was from a Laser-Vision optical parametric oscillator (OPO) pumped by a Nd:YAG laser (Continuum, Surelite-III-EX). The delay time between IR and UV laser pulses was varied in the 5–30 ns range. The UV and IR laser pulses were combined using a UV/IR dichroic mirror (Acton Optics). The chromatic aberration of UV and IR laser pulses was corrected by using a couple of the plano-convex lens in the UV laser beam path before combining two laser pulses. The IR and UV laser pulses then passed through a CaF_2 lens with a nominal focal length of 15 cm. In the velocity-map ion imaging (VMI[38,39]) setup, the polarizations of the two UV laser pulses were set to be parallel to a detector while the polarization of the IR laser pulse was orthogonal to that of the UV laser pulse. The position-sensitive detector equipped with a dual MCP (Burle, ϕ = 80 mm) and the P20 phosphor screen was used. A CCD camera (SONY XC-ST50) captured the images using the LABVIEW based acquisition program.[40] The center of the image was determined using the BASEX program,[41] while raw images were reconstructed using the MEVELER program.[42] The reconstructed images were calibrated according to the analysis of the VMI result from the O_2 dissociation dynamics.[39] The energy resolution of the UV laser pulse was $\sim$0.3 cm^{-1} whereas that of the OPO IR laser pulse was estimated to be $\sim$3.5 cm^{-1} when pumped with the Nd:YAG laser without the seed laser. Each VMI image contains accumulated events of at least 35 100 laser shots.

Results and discussion

In Fig. 1, the translational energy distribution of products from the S–H bond dissociation of CH_3SH has been obtained from the velocity-map ion images of the H fragment. As described above, we have employed the reduced-Doppler detection scheme[35] where the two counter-propagating laser pulses with different wavelengths of 268.84 and 221.92 nm were used for the H atom ionization. Therefore, the product state distributions (PSDs) at 268.84 and 221.92 nm are both reflected in the experiment. The low-kinetic energy portion of the distribution (PSD-A), which is sharp and asymmetric (15–22 kcal mol^{-1}), should originate from CH_3SH at 268.84 nm, whereas a rather wide distribution in the high-kinetic energy region (PSD-B) in the 30–45 kcal mol^{-1} region is attributed to that at 221.92 nm,

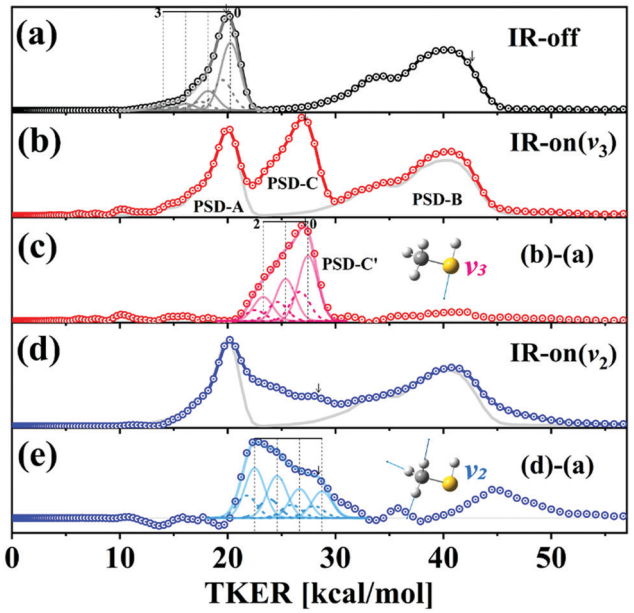

Fig. 1 Total kinetic energy release (TKER) distributions of products from the photodissociation of CH_3SH. (a) PSD from UV laser pulses of 268.84 (PSD-A) + 221.92 (PSD-B) nm. (b) PSD from the IR (ν_3 S–H stretch vibration; 2608 cm^{-1}) + UV excitation. (c) PSD-C′ from the IR (ν_3) + UV excitation only obtained from (b)–(a). (d) PSD from the IR (ν_3 C–H_3 symmetric stretch vibration; 2951 cm^{-1}) + UV excitation. (e) PSD from the IR (ν_2) + UV excitation only obtained from (d)–(a). PSD in (a) is shown as the gray line for the comparison. Vibrational quanta of the S–C stretching mode of 727 cm^{-1} (ref. 25) in two spin orbit states of the $CH_3S^{\bullet}$ radical are shown in (a) gray, (c) pink, and (e) light-blue as dashed ($E_{1/2}$) and solid ($E_{3/2}$). The partitioning ratio is estimated to be 97 or 90% for ν_3 or ν_2 vibration excitation in (c) or (e), respectively. The theoretically maximum kinetic energy is shown as black arrows. The ν_3 or ν_2 normal mode displacements (B3LYP with the 6-31g(d,p)) are shown in insets. The TKER distribution peaked at ~45 kcal mol^{-1} in (e) should come from the IR (ν_2) + UV (221.92 nm) excitation, which has not be discussed at the present time (ESI†).

Fig. 1(a). These PSDs are quite consistent with the previously reported results for both ~260 and ~220 nm cases.[25] PSD-A is well explained by the vibrational excitation of the C–S stretching mode at 727 cm^{-1} as well as the population of the excited spin–orbit states.[25] Though PSD-A in Fig. 1(a) is not vibrationally resolved, the simulation based on the C–S mode excitations of two spin–orbit $CH_3S^{\bullet}$ fragments explains the result quite well, providing the perfect consistency with the previously reported result obtained by the high-resolution Rydberg tagging method from the Ashfold group.[25] PSD-B is also consistent with the previous result reported by Wittig and colleagues.[20]

When the IR laser pulse is given for the excitation of the S–H stretching mode prior to the UV excitation, a new rather sharp peak appears between PSD-A and PSD-B, giving PSD-C, Fig. 1(b). The total energy given to CH_3SH is then either 37 197 (268.84 nm) + 2608 = 39 805 cm^{-1} (equivalent to a UV wavelength of ~251 nm) or 45 061 (221.92 nm) + 2608 = 47 669 cm^{-1} (~210 nm). As PSD-C is located higher but lower than PSD-A and -B, respectively, it should originate from the dissociation of CH_3SH at an IR + UV excitation of 37 197 (268.84 nm) + 2608 = 39 805 cm^{-1} (~251 nm). The PSD-C′ obtained by subtraction of the IR-off experiment from the IR-on experiment is then solely due to the IR + UV excitation, Fig. 1(c). PSD-C′ turns out to be almost identical to the PSD obtained by the one-photon UV excitation at ~251 nm.[20,27] This indicates that, in terms of PSD, the only difference between the one-photon UV excitation and the IR + UV double excitation is the oscillator strength if the total energy given to the system is identical. Namely, all of the S_0 internal energy given by the IR excitation is transferred to the translational energy of products (>97%), indicating that the subsequent UV vertical transition is shifted toward the shorter S–H bond length in the corresponding double excitation, Fig. 2. In the bound-to-repulsive transition, this is a rare occasion. This strongly indicates that the IVR is little activated at the S–H stretching mode excitation at 2608 cm^{-1} as the S_0 internal energy given by the IR transition would not otherwise go efficiently to the translational energy of products.

Although the S_1 state is repulsive along both S–H and S–C bond extensions in nature, it is still bound with respect to other internal degrees of freedom.[22–24] Thus, if the internally energized molecule by the IR excitation is followed by the rapid IVR in S_0, it will be FC active in the much wider volume of the phase space on the excited state upon the vertical UV excitation. This could lead to the slower release of products with the larger internal energy. Interestingly, when the CH_3 symmetric stretching mode is excited by IR as an optically bright state in the IR (2951 cm^{-1}) + UV (268.84 nm) double transition, the partitioning ratio of the available energy into the translational energy of the product is found to be only ~90% that expected when exciting $v = 0$ parent molecules with a single photon of the appropriate wavelength (~249 nm), Fig. 1(e). Instead, the internal energy distribution is found to be inverted, meaning that the $CH_3S^{\bullet}$ fragments of nonzero vibrational quantum

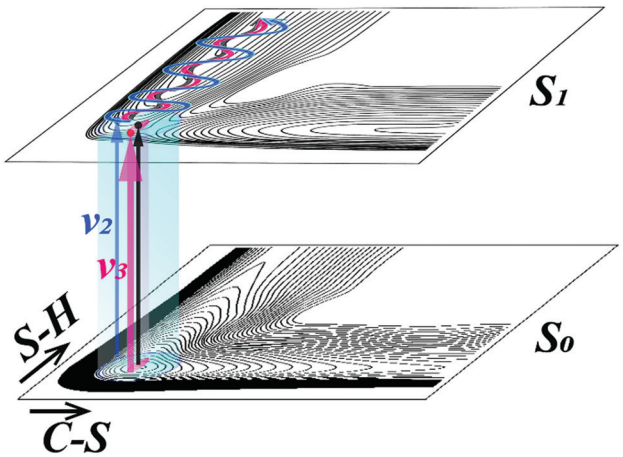

Fig. 2 The S_1 and S_0 potential energy surfaces of CH_3SH along the S–H and C–S elongation coordinates which are reproduced from ref. 26. Vertical transitions and associated energy disposal dynamics are shown in pink or blue lines when the IR + UV excitation is mediated (pink or cyan shades) by the S–H stretching mode (ν_3) or CH_3 symmetric stretching mode (ν_2), respectively (see the text). The black line shows the UV one-photon vertical transition from the zero-point level of the S_0 state. Reproduced from [*J. Chem. Phys.*, 1995, **102**, 7059; DOI: 10.1063/1.469099], with the permission of AIP Publishing.[26]

numbers are more populated than those of the ground state. From the PSD obtained by the difference between the IR-off and IR-on experiments, Fig. 1(e), it is obvious that the excited mode of the fragment is not likely due to the CH_3 symmetric stretching of $CH_3S^\bullet$ as it would otherwise be evident in terms of the energetic separation, indicating that the dissipative IVR may take place in the ground state. In this case, the subsequent UV vertical transition occurs from the internally hot S_0 states which are isoenergetic but dispersed along many degrees of freedom. This means that the FC region in the S_1 state could be enlarged in the IR + UV excitation *via* the CH_3 symmetric stretching mode due to the rapid IVR in S_0 as depicted in Fig. 2. As the energy disposal into products is determined by the exit shape of the potential energy surface, the vibrational mode excitation of the $CH_3S^\bullet$ fragment should also be associated with the C–S stretching mode as the repulsive S_1 along the S–H bond rupture is strongly coupled to the C–S extension (*vide supra*). It may be fair to state that the corresponding enlarged FC region now encompasses the nuclear structures where the C–S and S–H bond extensions in S_1 are more strongly coupled. Light and colleagues had calculated the S_0 and S_1 surfaces of CH_3SH with respect to both S–H and C–S bond elongation coordinates, Fig. 2.[26] According to them, the nuclear motions along those two coordinates are more strongly coupled in S_1 compared to S_0, which is at least conceptually consistent with our experimental results.

Conclusions

In summary, in the IR + UV excitation *via* the S–H stretching mode, the electronic vertical transition accesses the FC region where the S–H bond is shortened while its coupling to the C–S bond stretching is stronger compared to the one-photon UV excitation. In the IR + UV excitation *via* the CH_3 symmetric stretching mode, on the other hand, the vertically accessed FC region seems to encompass the S_1 molecular structures largely dispersed with respect to both S–H and C–S bond extensions due to the rapid IVR in S_0, leading to the inverted population of the C–S bond stretching vibrational excitation of the $CH_3S^\bullet$ fragment. The inverted vibrational excitation is likely to be associated with the inverted SH vibrational excitation observed in the C–S bond dissociation on S_2 ($2^1A''$) as the energy disposal dynamics along the C–S bond rupture should result from the strong coupling of S_1 and S_2 through the same-symmetry conical intersection.[22–24] The trajectory calculations on the sophisticated two-dimensional excited potential energy surfaces would be highly desirable for the better explanation of the present experiment. This work demonstrates that the IR + UV excitation of CH_3SH is highly mode dependent and the energy disposal dynamics could be controlled by the manipulation of the vertical transition by the vibrational mediation in the ground state, shedding new light on the structure–dynamics relationship.

Conflicts of interest

There are no conflicts to declare.

Acknowledgements

This work has been supported by the National Research Foundation (2018R1A2B3004534 and 2019K1A3A1A14064258).

References

1 R. L. Vander Wal, J. L. Scott and F. F. Crim, *J. Chem. Phys.*, 1990, **92**, 803–805.
2 T. M. Ticich, M. D. Likar, H. R. Dübal, L. J. Butler and F. F. Crim, *J. Chem. Phys.*, 1987, **87**, 5820–5829.
3 D. C. Tardy and B. S. Rabinovitch, *Chem. Rev.*, 1977, **77**, 369–408.
4 D. J. Nesbitt and R. W. Field, *J. Phys. Chem.*, 1996, **100**, 12735–12756.
5 D. Boyall and K. L. Reid, *Chem. Soc. Rev.*, 1997, **26**, 223–232.
6 A. Sinha, R. L. Vander Wal, L. J. Butler and F. F. Crim, *J. Phys. Chem.*, 1987, **91**, 4645–4647.
7 A. Sinha, R. L. Vander Wal and F. F. Crim, *J. Chem. Phys.*, 1989, **91**, 2929–2938.
8 R. L. Vander Wal and F. F. Crim, *J. Phys. Chem.*, 1989, **93**, 5331–5333.
9 M. Epshtein, A. Portnov, S. Rosenwaks and I. Bar, *J. Chem. Phys.*, 2011, **134**, 201104.
10 A. Golan, S. Rosenwaks and I. Bar, *J. Chem. Phys.*, 2006, **125**, 151103.
11 F. F. Crim, *Annu. Rev. Phys. Chem.*, 1993, **44**, 397–428.
12 I. Bar and S. Rosenwaks, *Int. Rev. Phys. Chem.*, 2001, **20**, 711–749.
13 S. Rosenwaks, *Vibrationally Mediated Photodissociation*, The Royal Society of Chemistry, 2009, pp. 1–8, DOI: 10.1039/9781847558176-00001.
14 M. L. Hause, Y. Heidi Yoon, A. S. Case and F. F. Crim, *J. Chem. Phys.*, 2008, **128**, 104307.
15 K. Grygoryeva, J. Rakovský, I. S. Vinklárek, O. Votava, M. Fárník and V. Poterya, *AIP Adv.*, 2019, **9**, 035151.
16 M. Xie, Z. Shen, S. T. Pratt and Y.-P. Lee, *Phys. Chem. Chem. Phys.*, 2017, **19**, 29153–29161.
17 G. P. Sturm and J. M. White, *J. Chem. Phys.*, 1969, **50**, 5035–5036.
18 J. S. Keller, P. W. Kash, E. Jensen and L. J. Butler, *J. Chem. Phys.*, 1992, **96**, 4324–4329.
19 E. Jensen, J. S. Keller, G. C. G. Waschewsky, J. E. Stevens, R. L. Graham, K. F. Freed and L. J. Butler, *J. Chem. Phys.*, 1993, **98**, 2882–2890.
20 J. Segall, Y. Wen, R. Singer, M. Dulligan and C. Wittig, *J. Chem. Phys.*, 1993, **99**, 6600–6606.
21 G. L. Vaghjiani, *J. Chem. Phys.*, 1993, **99**, 5936–5943.
22 J. E. Stevens, K. F. Freed, M. F. Arendt and R. L. Graham, *J. Chem. Phys.*, 1994, **101**, 4832–4841.
23 D. R. Yarkony, *J. Chem. Phys.*, 1994, **100**, 3639–3644.
24 D. R. Yarkony, *J. Chem. Phys.*, 1996, **104**, 7866–7881.
25 S. H. S. Wilson, M. N. R. Ashfold and R. N. Dixon, *J. Chem. Phys.*, 1994, **101**, 7538–7547.
26 J. E. Stevens, H. W. Jang, L. J. Butler and J. C. Light, *J. Chem. Phys.*, 1995, **102**, 7059–7069.

27 L. J. Rogers, M. N. R. Ashfold, Y. Matsumi, M. Kawasaki and B. J. Whitaker, *J. Chem. Soc., Faraday Trans.*, 1996, **92**, 5181–5183.
28 J. G. Izquierdo, G. A. Amaral, F. Ausfelder, F. J. Aoiz and L. Bañares, *ChemPhysChem*, 2006, **7**, 1682–1686.
29 G. A. Amaral, F. Ausfelder, J. G. Izquierdo, L. Rubio-Lago and L. Bañares, *J. Chem. Phys.*, 2007, **126**, 024301.
30 Z. Chen, Q. Shuai, A. T. J. B. Eppink, B. Jiang, D. Dai, X. Yang and D. H. Parker, *Phys. Chem. Chem. Phys.*, 2011, **13**, 8531–8536.
31 D. V. Chicharro, S. Marggi Poullain, L. Rubio-Lago and L. Bañares, *J. Phys. Chem. A*, 2019, **123**, 8552–8561.
32 J. S. Lim and S. K. Kim, *Nat. Chem.*, 2010, **2**, 627–632.
33 J.-H. Yoon, K. C. Woo and S. K. Kim, *Phys. Chem. Chem. Phys.*, 2014, **16**, 8949–8955.
34 A. E. Pomerantz and R. N. Zare, *Chem. Phys. Lett.*, 2003, **370**, 515–521.
35 C. Huang, W. Li, M. Hwa Kim and A. G. Suits, *J. Chem. Phys.*, 2006, **125**, 121101.
36 J. S. Lim, H. Choi, I. S. Lim, S. B. Park, Y. S. Lee and S. K. Kim, *J. Phys. Chem. A*, 2009, **113**, 10410–10416.
37 M. Epshtein, A. Portnov, R. Kupfer, S. Rosenwaks and I. Bar, *J. Chem. Phys.*, 2013, **139**, 184201.
38 D. W. Chandler and P. L. Houston, *J. Chem. Phys.*, 1987, **87**, 1445–1447.
39 A. T. J. B. Eppink and D. H. Parker, *Rev. Sci. Instrum.*, 1997, **68**, 3477–3484.
40 W. Li, S. D. Chambreau, S. A. Lahankar and A. G. Suits, *Rev. Sci. Instrum.*, 2005, **76**, 063106.
41 V. Dribinski, A. Ossadtchi, V. A. Mandelshtam and H. Reisler, *Rev. Sci. Instrum.*, 2002, **73**, 2634–2642.
42 B. Dick, *Phys. Chem. Chem. Phys.*, 2014, **16**, 570–580.